Iranian Journal of Organic Chemistry Vol. 9, No. 1 (2017) 2001-2012

Theoretical studies of molecular structure of natural products: Acromelic acid A and B

Mousa Soleymani*

Department of Chemistry, Faculty of Basic Science, University of Ayatollah Alozma Borujerdi, Borujerd 69199-69411, Iran

Received: November 2016; Revised: December 2016; Accepted: January 2017

Abstract: The computational methods were used for investigation of structural, electronic and bonding characteristics of acromelic acid A and B. The results of AIM calculations with those obtained from potential energy surfaces analysis and optimizations calculations indicated that several factors such as steric hindrances, intra-molecular hydrogen bond and possibility of resonance interaction of some functional groups with adjacent π-bond, affect the structural parameters and the stability of conformations of acromelic acid A and B.

Keywords: Acromelic acid, Potential Energy Surface (PES), Conformational analysis, AIM analysis.

Introduction

The kainoids (non-proteinogenic amino acids) are a group of pyrrolidine derivatives that occurs naturally. Being the three stereogenic centers on the pyrrolidine ring (from C_2 to C_4), is one of the interesting features of these compounds. The π-system substituent located on 4 position of the pyrrolidine ring can vary in nature. Two typical examples of kainoids are constructional isomeric forms of acromelic acid, namely, acromelic acid A (**AA**) and acromelic acid B (**AB**). These compounds were first found in the poisonous Japanese mushroom, *Clitocybeacromelalga* [1]. Generally in all members of kainoids family, the *S*-absolute configuration of C_2 and a *trans* geometry of its substituent with respect to the adjacent substituent on C_3 has been observed. With the exception of allokainic acid, in allkainoids, substituents located on C_3 and C_4 atoms have a *cis* configuration [2-4].

*Corresponding author. Tel.:(+98) 6642468320, Fax: (+98) 6642468223, E-mail: m_soleymani2007@yahoo.com

Kainoids exhibit considerably potent neuro-excitatory activity via activation of ionotropic glutamate receptors in the brain. These compounds have the potential to be important biological research tools, because ionotropic glutamate receptors are involved in various neurophysiological processes, including memory and learning [5]. Thus various research works were devoted to the synthesis and investigation of their biological aspects [6-13]. Other derivatives of acromelic acids were also synthesized and their biological activities were investigated. For example analogue of these amino acids with ^{13}C label were synthesized for detection of the site of action of acromelic acid A on tactile pain [8]. Acromelic acids analogue containing a phenyl group with two different types of azido (N_3) groups, were synthesized and investigated for radioisotope-free photoaffinity labeling and biochemical studies [9]. Because of the effect of molecular geometry and other structural parameters on the biological activities, the theoretical studies of these compounds may be subject of interest.

In continuation of our theoretical studies concerning various organic compounds [14,15], and since there is

not found comprehensive theoretical researches concerning these compounds in literatures, we applied B3LYP/6-31++G**, M052X/6-31++G** and AIM methods to study structural, electronic and thermodynamic aspects of **AA** and **AB** compounds. The optimization calculations were carried out in both gas phase and aqueous solution (using CPCM method). The aims of the present work are:

- To elucidate the effect of heterocyclic group located on the 4 position of pyrrolidine ring on the structural, electronic and thermodynamic parameters of the molecule.
- To elucidate the effect of solvation on the structural parameters.
- To Study of the stability of tautomeric forms of heterocycle ring located on C_4.
- AIM calculations for studies of the intra-molecular interactions especially hydrogen bonds.
- Potential Energy Surface (PES) calculations for conformational analysis to obtain lowest and highest energy conformers.

Results and Discussion

Structural analysis:

Figure **1** shows the optimized structures of acromelic acids in gas phase and aqueous solution.

As can be seen, the five-membered heterocyclic ring, pyrrolidine core, in **AA** adopts an *envelope* conformation which approximately flatted at C_2-N_1-C_5-C_4 plane with a *pseudoequatorial* orientation of the C_3-substituent. The C_2-N_1-C_5-C_4 dihedral angles in gas phase and aqueous solution have a value of 1.19° and 1.29°, respectively, which is consistent with above mentioned geometry. A similar conformation was found for **AB** with the exception that the five-membered ring flatted at N_1-C_2-C_3-C_4 plane and deviated from this plane at C_5 so that the value of N_1-C_2-C_3-C_4 dihedral angle for **AB** compound in gas phase and aqueous solution are 0.35° and 0.82°, respectively. These two different geometries can be attributed to the difference in the position of functional groups on pyridone ring located on C_4, which leads to the different intra-molecular interactions.

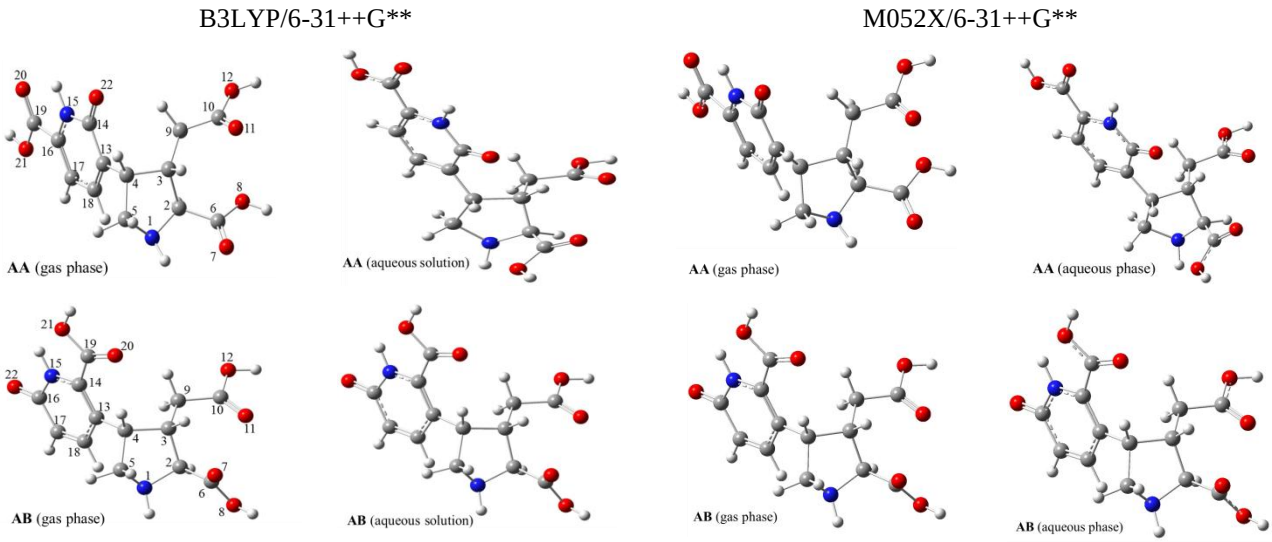

Figure 1: Optimized structures of **AA** and **AB** in gas phase and aqueous solution obtained by B3LYP/6-31++G**and M052X/6-31++G** methods**.**

The optimized values of the bond lengths, bond angles: C_5-N_1-C_2 (a), N_1–C_2–C_6 (b), N_1-C_2-C_3 (c), C_2–C_6–O_7 (d),C_9–C_{10}–O_{11} (e), dihedral angles: N_1–C_2–C_3–C_4 (f), N_1–C_2–C_6–O_7 (g), C_2–C_3–C_4–C_5 (h), C_2–C_3–C_9–C_{10} (i), C_3–C_9–C_{10}–O_{11} (j) and C_3–C_4–C_{13}–C_{18} (k)of acromelic acids obtained by using M052X/6-31++G** and B3LYP/6-31++G** methods are listed in Tables **1** and Table **S1** of supporting information, respectively. Other structural parameters are summarized in Table **S2** and **S3**.

Analysis of the data reported in Table **1** (and Table **S1**) indicates that:

Because of several polar functional groups such as NH, C=O and COOH on both heterocyclic rings of **AA** and

AB, which resulting hydrogen bond formation between these polar functional groups and water molecules, partial changes (especially for **AA**) in the molecular geometry are observed in aqueous solution in comparison to gas phase.

Table 1: Some selected bond lengths (in Å), bond angles and dihedral angles (in °), for **AA** and **AB** compounds obtained by M052X/6-31++G** level of theory.

Comp.	C_6-O_7	C_6-O_8	O_8-H	N_1-H	C_2-H	C_3-H	C_4-H	C_5-H	C_5-H'	C_9-H
AA$_{(g)}$	1.2073	1.3446	0.9684	1.0123	1.0967	1.0939	1.0907	1.0947	1.0919	1.0953
AA$_{(aq)}$	1.2129	1.3392	0.9701	1.0096	1.0929	1.0873	1.0955	1.0912	1.0918	1.0944
AB$_{(g)}$	1.2091	1.3495	0.9682	1.0123	1.0911	1.0903	1.0852	1.0963	1.0923	1.0922
AB$_{(aq)}$	1.2135	1.3407	0.9698	1.0127	1.0912	1.0900	1.0849	1.0960	1.0916	1.0922
Comp.	C_9-H'	C_{10}-O_{11}	C_{10}-O_{12}	O_{12}-H	C-O_{22}	C_{19}-O_{20}	C_{19}-O_{21}	O_{21}-H	N_{15}-H	*a*
AA$_{(g)}$	1.0925	1.2089	1.3468	0.9678	1.2293	1.2095	1.3389	0.9679	1.0137	108.78
AA$_{(aq)}$	1.0931	1.2126	1.3423	0.9696	1.2377	1.2128	1.3301	0.9698	1.0140	109.46
AB$_{(g)}$	1.0948	1.2098	1.3460	0.9681	1.2246	1.2088	1.3486	0.9680	1.0107	107.53
AB$_{(aq)}$	1.0942	1.2143	1.3400	0.9696	1.2391	1.2106	1.3388	0.9700	1.0121	107.64
Comp.	*b*	*c*	*d*	*e*	*f*	*g*	*h*	*i*	*j*	*k*
AA$_{(g)}$	111.80	105.93	125.22	125.98	-31.61	-20.92	42.41	-85.03	-19.71	88.97
AA$_{(aq)}$	116.05	103.69	123.37	125.97	41.49	178.50	-40.30	-72.93	-7.79	113.93
AB$_{(g)}$	109.97	104.94	125.11	125.52	0.35	-77.15	22.28	-62.06	3.85	84.63
AB$_{(aq)}$	110.17	105.05	125.36	125.24	0.8240	-79.44	22.54	-62.86	2.13	85.50

1) The greater change observed in the conformation of **AA** in aqueous solution relative to gas phase probably can be attributed to the mediation role of the water molecule between O_7 and O_{11} atoms of two carboxyl groups for the formation of inter-molecular hydrogen bond. The distance of two relevant oxygens (O_7…O_{11}) is 3.87 Å, which is favored for this interaction. For compound **AB** in gas phase, due to proper orientation of carboxyl groups for the formation of similar inter-molecular interaction in aqueous solution, a drastic change in the geometry has not been observed and the structural deviations is less than to **AA**.
2) In all cases the bond length of O−H bonds in aqueous solution is partially greater than its value in gas phase. In other words the O−H bonds in solution phase are weaker relative to gas phase. This can be attributed to the formation of inter-molecular hydrogen bond with H_2O molecules in solution phase.
3) Due to three stereo centers at C_2, C_3 and C_4 atoms, the bond lengths of diastereotopic hydrogen pairs attached to C_5 and C_9 atoms are different.
4) According to the optimized structures, it can be concluded that in contrast to the N_1-H bond, the N_{15}–H bond is coplanar with respect to the heterocyclic ring which is supported by hybridization data obtained by NBO calculation, so that the calculated hybridizations of N_1 and N_{15} for compound **AA** in gas phase are $sp^{2.83}$ and $sp^{2.52}$, respectively and those for **AB** are $sp^{2.91}$ and $sp^{2.52}$, respectively.

NBO charges, standard enthalpies of formation (ΔH_f°), standard Gibbs free energies of formation (ΔG_f°), total energy (E), E_{HOMO}, E_{LUMO} and global hardness (η) of acromelic acids are listed in Table **2**.

A comparison of the results presented in Table **2** indicates that:

1) Total energy (E) and thermodynamic parameters (standard enthalpies of formation (ΔH_f°) and standard Gibbs free energies of formation (ΔG_f°)) in solution phase are lower relative to gas phase which can be attributed to the solvation effects.

Table 2: NBO charges, standard formation enthalpies (ΔH_f° , in kJ.mol^{-1}), standard formation Gibbs free energies **(** ΔG_f° , in kJ.mol^{-1}**)**, E (in a. u.), E_{HOMO} (in a. u.), E_{LUMO} (in a. u.) and hardness (η) of **AA** and **AB** compounds obtained by M052X/6-31++G** and B3LYP/6-31++G** methods.

Comp.[a]	*N_1*	N_1*H*	*O_7*	*O_8*	O_8*H*	*O_{11}*	*O_{12}*	O_{12}*H*	*N_{15}*	N_{15}*H*
AA$_{(g)}$	-0.737	0.428	-0.624	-0.732	0.530	-0.640	-0.730	0.522	-0.586	0.477
AA$_{(aq)}$	-0.737	0.427	-0.666	-0.734	0.544	-0.664	-0.735	0.539	-0.575	0.481
AB$_{(g)}$	-0.721	0.413	-0.636	-0.726	0.523	-0.632	-0.729	0.524	-0.601	0.472
AB$_{(aq)}$	-0.725	0.424	-0.671	-0.731	0.538	-0.666	-0.731	0.540	0.583	0.480
Comp.[a]	*O_{20}*	*O_{21}*	O_{21}*H*	*O_{22}*	ΔH_f°	ΔG_f°	E	E_{HOMO}	E_{LUMO}	η
AA$_{(g)}$	-0.615	-0.718	0.534	-0.666	-782.98	-202.43	-1139.90	-0.2957	-0.0587	0.1185
AA$_{(aq)}$	-0.643	-0.714	0.552	-0.718	-844.90	-272.33	-1139.92	-0.2952	-0.0524	0.1214
AB$_{(g)}$	-0.610	-0.738	0.538	-0.651	-747.92	-169.12	-1139.88	-0.2893	-0.0568	0.1163
AB$_{(aq)}$	-0.629	-0.732	0.555	-0.731	-827.05	-248.70	-1139.91	-0.2912	-0.0517	0.1198
Comp.[b]	*N_1*	N_1*H*	*O_7*	*O_8*	O_8*H*	*O_{11}*	*O_{12}*	O_{12}*H*	*N_{15}*	N_{15}*H*
AA$_{(g)}$	-0.725	0.419	-0.611	-0.716	0.515	-0.620	-0.717	0.515	-0.574	0.467
AA$_{(aq)}$	-0.726	0.421	-0.649	-0.720	0.537	-0.648	-0.722	0.533	-0.563	0.470
AB$_{(g)}$	-0.707	0.406	-0.616	-0.715	0.516	-0.612	-0.718	0.517	-0.588	0.463
AB$_{(aq)}$	-0.709	0.417	-0.653	-0.718	0.531	-0.649	-0.720	0.533	0.571	0.470
Comp.[b]	*O_{20}*	*O_{21}*	O_{21}*H*	*O_{22}*	ΔH_f°	ΔG_f°	E	E_{HOMO}	E_{LUMO}	η
AA$_{(g)}$	-0.603	-0.706	0.526	-0.650	-1392.09	-1057.66	-1140.02	-0.2379	-0.0976	0.0702
AA$_{(aq)}$	-0.632	-0.702	0.544	-0.704	-1454.14	-1127.80	-1140.04	-0.2055	-0.1260	0.0398
AB$_{(g)}$	-0.596	-0.727	0.531	-0.635	-1358.04	-1027.63	-1140.00	-0.2160	-0.1376	0.0392
AB$_{(aq)}$	-0.617	-0.721	0.548	-0.717	-1434.85	-1104.63	-1140.03	-0.2064	-0.1302	0.0381

[a,b] The results obtained from B3LYP/6-31++G** and M052X/6-31++G** methods, respectively.

2) Since **AA** and **AB** compounds are structural isomers, the standard enthalpies of formation, standard Gibbs free energies of formation and global hardness may be applied for comparison of their stabilities. The results indicate that **AA** is more stable relative to its isomer which can be justified on the basis of the less steric repulsions of the pyridone ring with adjacent atoms or groups.

3) The analysis of NBO charges indicate that due to the delocalization of unpaired electron on N_{15} (which is cross-conjugated with adjacent carbonyl group) and diene system of 2-pyridone, its negative charge is lower relative to N_1 atom. Owing to this conjugation the negative charge on O_{22} atom is greater than to the other oxygens of carboxyl groups (C=O_7, C=O_{11} and C=O_{20}).

Since amino acids have one or more proton donating groups (COOH) and proton accepting groups (-NR_2, -NH_2 or -NHR), the formation of zwitterion is possible in crystalline form, aqueous solution and even in gas phase [16,17]. In acromelic acids three zwitterions may be formed due to the possibility of three proton transfer from three carboxyl groups to N_1 atom. The optimized structures of these species are illustrated in Figures **S1** and **S2** of supplementary materials. For determination of more favorable zwitterion, their thermodynamic parameters were calculated in aqueous solution. The results are presented in Table **S4** of supplementary materials. A comparison of these results indicates that the zwitterions (**AA-I** and **AB-I**) produced by proton transfer from O_8 to N_1 is energetically lower relative to others. This stability can be attributed to the formation of intra-molecular hydrogen bond (between the oxygen atoms of carboxylate ion with hydrogen atom attached to N_1) via a cyclic five-membered arrangement. The resulted N_1H…O hydrogen bond has a length of 1.75-1.78 Å which is less than the sum of van der Waals radii of hydrogen and oxygen atoms (2.72 Å). Figures

S1 and **S2** are also illustrated the corresponding intra-molecular hydrogen bond lengths and energies, which the later calculated according to the Espinosa equation [18].

For investigations of intra-molecular charge transfer or donor-acceptor interactions, NBO analysis (Second Order Perturbation Theory Analysis of Fock Matrix in NBO Basis) can be used. Results of NBO analysis performed on **AA** and **AB** are summarized in Table **3**. Second order stabilization energies E(2) provide a satisfactory criterion for donor-acceptor interactions [19]. A greater value of E(2)indicates a higher degree of electrons delocalization.

Table 3: Second order stabilization energies (E(2) in kcal.mol^{-1}) for donor-acceptor interactions of **AA** and **AB** obtained by NBO analysis.

Comp.	Donor	Acceptor	B3LYP/6-31++G**		M052X/6-31++G**	
			E(2)	ΣE(2)	E(2)	ΣE(2)
AA(g)	LP (N_1)	σ*(C_2–H)	4.87	4.87	6.09	6.09
AA(g)	LP (N_1)	σ*(C_2–C_3)	2.25	2.25	3.36	3.36
AA(g)	LP (N_1)	σ*(C_5–H)	8.15	8.15	9.23	9.23
AA(g)	LP (N_1)	σ*(C_2–C_6)	2.09	2.09	1.94	1.94
AA(g)	LP (N_1)	σ*(C_{18}–H)	1.50	1.50	1.86	1.86
AA(g)	LP (O_8)	σ*(C_6=O_7)	8.65	55.41	10.04	68.43
AA(g)	LP (O_8)	π*(C_6=O_7)	46.76		58.39	
AA(g)	LP (O_{12})	σ*(C_{10}=O_{11})	8.21	52.69	9.62	66.81
AA(g)	LP (O_{12})	π*(C_{10}=O_{11})	44.48		57.19	
AA(g)	LP (N_{15})	π*(C_{14}=O_{22})	55.91	55.91	75.13	75.13
AA(g)	LP (N_{15})	π*(C_{16}=C_{17})	42.25	42.25	54.60	54.60
AA(g)	LP (O_{21})	σ*(C_{19}=O_{20})	8.46	55.45	9.89	70.00
AA(g)	LP (O_{21})	π*(C_{19}=O_{20})	46.99		60.11	
AB(g)	LP (N_1)	σ*(C_2–H)	2.90	2.90	3.67	3.67
AB(g)	LP (N_1)	σ*(C_5–H)	8.29	8.29	9.62	9.62
AB(g)	LP (N_1)	σ*(C_2–C_6)	5.88	5.88	6.96	6.96
AB(g)	LP (N_1)	π*(C_6=O_7)	2.33	2.33	2.78	2.78
AB(g)	LP (N_1)	σ*(C_{18}–H)	2.69	2.69	3.26	3.26
AB(g)	LP (O_8)	σ*(C_6=O_7)	8.55	55.04	10.09	69.88
AB(g)	LP (O_8)	π*(C_6=O_7)	46.49		59.79	
AB(g)	LP (O_{12})	σ*(C_{10}=O_{11})	8.35	55.15	9.85	69.40
AB(g)	LP (O_{12})	π*(C_{10}=O_{11})	46.80		59.55	
AB(g)	LP (N_{15})	π*(C_{16}=O_{22})	53.22	53.22	71.19	71.19
AB(g)	LP (N_{15})	π*(C_{13}=C_{14})	39.97	39.97	51.70	51.70
AB(g)	LP (O_{21})	σ*(C_{19}=O_{20})	7.71	51.71	9.14	65.89
AB(g)	LP (O_{21})	π*(C_{19}=O_{20})	44.00		56.75	
AB(g)	LP (O_{21})	σ*(N_{15}–H)	1.87	1.87	1.92	1.92

The results reported in Table **3** indicate that in comparison to N_1 atom, the N_{15} atom is a better donor because of conjugation of its unpaired electrons with adjacent π systems. Also among the oxygen atoms conjugated with carbonyl groups, in **AA,** O_{21} has more character of σ or π donating effect to the adjacent C_{19}=O_{20} carbonyl group, while in **AB**, O_8 and O_{12} atoms have more donating effect. The results are summarized in Table **4**.

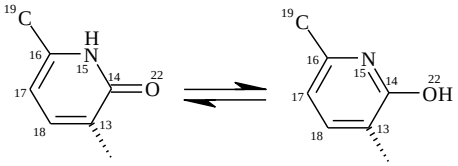

Acromelic acid A

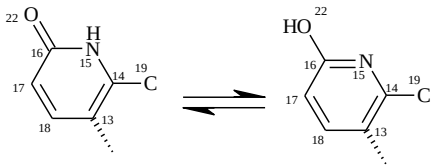

Acromelic acid B

Tautomeric effect:

The heterocyclic ring at the 4 position of pyrollidine ring of **AA** and **A**B may be exits in two equilibrium tautomeric forms: 2-pyridone and aromatic 2-hydroxy pyridine (lactam lactim tautomerism) [20,21]. For comparison of those stabilities, the standard Gibbs free energies ΔG°_{r} and equilibrium constants K_e of the following reactions were calculated in gas phase and aqueous solution. These results clearly indicate that 2-pyridone is more stable relative to 2-hydroxypyridine and almost is the only tautomeric form of Acromelic acid in either gas phase or aqueous solution.

AIM analysis:

For investigation of the energies and nature of intra-molecular hydrogen bond, topological parameters at bond critical points (BCP) were calculated by theory of Atoms In Molecule (AIM). By formation of hydrogen bond the electron density distribution will be changed and we can obtain some information concerning about that by using AIM theory. Figure **2** shows the molecular graphs of **AA** and **AB** in both gas phase and aqueous solution obtained by AIM program. The topological parameters are summarized in Table **5**. For estimation of hydrogen bond energy the Espinosa equation was used [18]. A review of the data presented in Table **5** indicates that:

Table 4: Calculated standard Gibbs free energies and equilibrium constants for lactam lactim tautomerisation reactions of **AA** and **AB**.[a]

Comp.	2-pyridone		2-hydroxy pyridine		ΔG°_{r}	ΔE_{tot}	K_e
	ΔG°_{f}	$\mathbf{E_{tot}}$	ΔG°_{f}	$\mathbf{E_{tot}}$			
AA(g)[b]	-1057.66	−2993113.97	-1037.88	−2993091.88	+19.78	+22.09	3.42×10^{-4}
AA(aq)[b]	-1127.80	−2993173.39	-1107.76	−2993150.47	+20.04	+22.92	3.08×10^{-4}
AB(g)[b]	-1027.63	−2993079.54	-1000.42	−2993051.07	+27.21	+28.47	1.71×10^{-5}
AB(aq)[b]	-1104.63	−2993154.41	-1080.72	−2993128.43	+23.91	+25.98	6.47×10^{-5}
AA(g)[c]	-202.43	-2992795.69	-192.80	-2992783.37	+9.63	+12.32	2.05×10^{-2}
AA(aq)[c]	-272.33	-2992853.79	-259.73	-2992841.03	+12.60	+12.76	6.20×10^{-3}
AB(g)[c]	-169.12	-2992760.45	-151.36	-2992742.68	+17.76	+17.77	7.73×10^{-4}
AB(aq)[c]	-248.70	-2992837.10	-236.08	-2992822.28	+12.62	+14.82	6.18×10^{-3}

[a] All energies are in $kJ.mol^{-1}$.
[b,c] The results obtained from B3LYP/6-31++G** and M052X/6-31++G** methods, respectively.

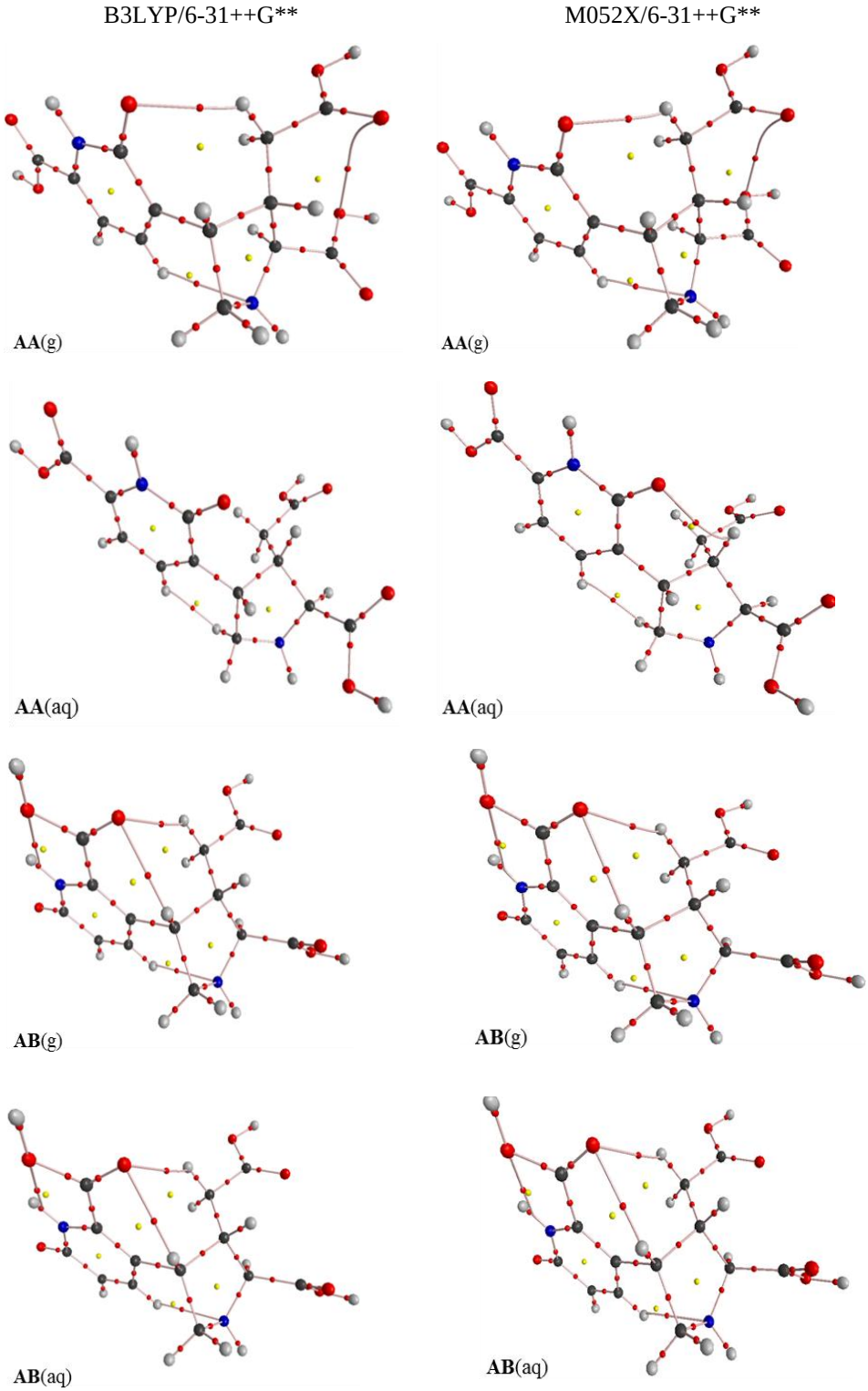

Figure 2: Molecular graphs of **AA** and **AB** in both gas phase and aqueous solution obtained by AIM program (bond critical points (red spheres), ring critical points (small yellow sphere), bond paths (pink lines)).

1) In all cases, the distance between interacting atoms (d) is less than the sum of van der Waals radii (2.75 and 2.72 Å for r_N+r_H and r_O+r_H, respectively), which is resulted intra-molecular hydrogen bond formation.

2) In the case of compound **AA**, in contrast to gas phase, for aqueous solution calculations the corresponding intra-molecular interactions are diminished. This may be attributed to the distance increment of interacting atoms and also increasing the possibility of interactions of functional groups with water molecules.

3) Since the structure of **AB** in both gas and solution phases is very similar, four similar interactions were found in both cases, but due to interaction with water molecules in aqueous solution, the intra-molecular hydrogen bond energies (E_{HB}) are reduced.

4) For either **AA** or **AB** in gas phase, the O…H−O hydrogen bond is not observed. It may be concluded that inter-molecular hydrogen bond with water molecules in aqueous solution is responsible of increment of O−H bond lengths (Table **1**).

Potential Energy Surface (PES) analysis

PES scan of **AA** and **AB** was performed around five different selected dihedral angles with 10° increment. The potential energy curves of **AA** and AB were plotted as a function of C_2–C3–C_9–C_{10} (α), C_3–C_9–C_{10}–O_{11} (β), C_3–C_2–C_6–O_7 (γ), C_5–C_4–C_{13}–C_{18} (φ) and $C_{17(or13)}$–$C_{16(or14)}$–C_{19}–O_{20} (θ) dihedral angles which is illustrated in Figure **3**. As shown in Figure **3**, the internal rotation around selected bond, yielded several maximum and minimum points on the potential energy surface curves. The stability or instability of conformers is dependent to some factors such as steric and electronic (polar) effects. Attractive (especially hydrogen bond) or repulsive interactions and steric hindrances play an important role on the stability or instability of conformers. Since **AA** and **AB** have several polar functional groups, intra-molecular hydrogen bond formation is affected the stability of conformers. Along with the PES curves, the geometries corresponding to the minimum or maximum points shown in Figure **3**.

Table 5. Topological parameters of intra-molecular hydrogen bond for **AA** and **AB** in both gas phase and aqueous solution obtained by AIM calculations: electron density ρ_{BCP} and corresponding Laplacian$\nabla^2\rho_{BCP}$, electronic kinetic energy density G_{BCP}, electronic potential energy density V_{BCP}, electronic energy density H_{BCP} and estimated hydrogen bond energy E_{HB} at bond critical point BCP. [a]

Comp.	Interaction	ρ_{BCP}	$\nabla^2\rho_{BCP}$	G_{BCP}	V_{BCP}	H_{BCP}	E_{HB}	d [b]
AA(g)[c]	N_1…H−C_{18}	1.2481×10^{-2}	4.0404×10^{-2}	9.0076×10^{-3}	7.9140×10^{-3}	1.6922×10^{-2}	10.39	2.46
AA(g)[c]	C_9–H …O_{22}	1.0751×10^{-2}	3.5406×10^{-2}	8.0873×10^{-3}	7.3230×10^{-3}	1.5410×10^{-2}	9.61	2.44
AB(g)[c]	N_1…H–C_{18}	1.6247×10^{-2}	4.8473×10^{-2}	1.1346×10^{-2}	1.0575×10^{-2}	2.1921×10^{-2}	13.88	2.34
AB(g)[c]	C_4–H…O_{20}	1.7804×10^{-2}	6.2376×10^{-2}	1.4399×10^{-2}	1.3205×10^{-2}	2.7604×10^{-2}	17.33	2.22
AB(g)[c]	C_9–H …O_{20}	5.8618×10^{-3}	2.1619×10^{-2}	4.5041×10^{-3}	3.6034×10^{-3}	8.1075×10^{-2}	4.73	2.73
AB(g)[c]	N_{15}–H…O_{21}	1.8703×10^{-2}	8.6927×10^{-2}	1.8590×10^{-2}	1.5448×10^{-2}	3.4038×10^{-2}	20.28	2.16
AB(aq)[c]	N_1…H−C_{18}	1.5073×10^{-2}	4.5394×10^{-2}	1.0515×10^{-2}	9.6816×10^{-3}	2.0197×10^{-2}	12.71	2.38
AB(aq)[c]	C_4–H…O_{20}	1.7356×10^{-2}	6.0954×10^{-2}	1.4022×10^{-2}	1.2806×10^{-2}	2.6828×10^{-2}	16.81	2.24
AB(aq)[c]	C_9–H …O_{20}	5.6315×10^{-3}	2.0914×10^{-2}	4.3300×10^{-3}	3.4315×10^{-3}	7.7615×10^{-3}	4.50	2.76
AB(aq)[c]	N_{15}–H…O_{21}	1.8881×10^{-2}	8.7448×10^{-2}	1.8739×10^{-2}	1.5616×10^{-2}	3.4355×10^{-2}	20.50	2.15
AA(g)[d]	N_1…H−C_{18}	1.3768×10^{-2}	4.5099×10^{-2}	1.0301×10^{-2}	9.3269×10^{-3}	1.9628×10^{-2}	12.24	2.41
AA(g)[d]	C_9–H …O_{22}	1.2056×10^{-2}	4.0164×10^{-2}	9.3455×10^{-3}	8.6499×10^{-3}	1.7995×10^{-2}	11.36	2.39
AA(aq)[d]	C_3–H …O_{22}	1.0377×10^{-2}	3.8750×10^{-2}	8.4322×10^{-3}	7.1769×10^{-3}	1.5609×10^{-2}	9.42	2.57
AB(g)[d]	N_1…H–C_{18}	1.7683×10^{-2}	5.3092×10^{-2}	1.2776×10^{-2}	1.2278×10^{-2}	2.5054×10^{-2}	16.12	2.30
AB(g)[d]	C_4–H…O_{20}	1.7655×10^{-2}	6.4220×10^{-2}	1.4747×10^{-2}	1.3439×10^{-2}	2.8186×10^{-2}	17.64	2.24

AB(g)[d]	C_9–H …O_{20}	8.9555×10^{-3}	3.1430×10^{-2}	7.0166×10^{-3}	6.1757×10^{-3}	1.3192×10^{-2}	8.11	2.53
AB(g)[d]	N_{15}–H…O_{21}	1.8901×10^{-2}	9.1687×10^{-2}	1.9578×10^{-2}	1.6234×10^{-2}	3.5812×10^{-2}	21.31	2.17
AB(aq)[d]	N_1…H–C_{18}	1.6846×10^{-2}	5.0982×10^{-2}	1.2173×10^{-2}	1.1600×10^{-2}	2.3773×10^{-2}	15.23	2.33
AB(aq)[d]	C_4–H…O_{20}	1.7284×10^{-2}	6.2976×10^{-2}	1.4414×10^{-2}	1.3085×10^{-2}	2.7499×10^{-2}	17.18	2.26
AB(aq)[d]	C_9–H …O_{20}	9.1263×10^{-3}	3.1886×10^{-2}	7.1426×10^{-3}	6.3137×10^{-3}	1.3456×10^{-2}	8.29	2.52
AB(aq)[d]	N_{15}–H…O_{21}	1.9112×10^{-2}	9.2388×10^{-2}	1.9770×10^{-2}	1.6444×10^{-2}	3.6214×10^{-2}	21.59	2.16

[a] ρ_{BCP}, $\nabla^2\rho_{BCP}$, G_{BCP}, V_{BCP}, H_{BCP} in a.u. and E_{HB} in kJ.mol^{-1}.
[b]The distance between interacting atoms in Angstrom.
[c,d]The results obtained from wave function of B3LYP/6-31++G** and M052X/6-31++G** methods, respectively.

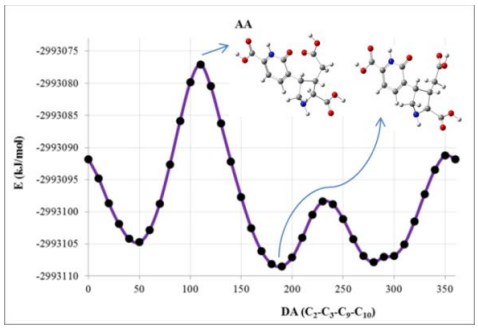

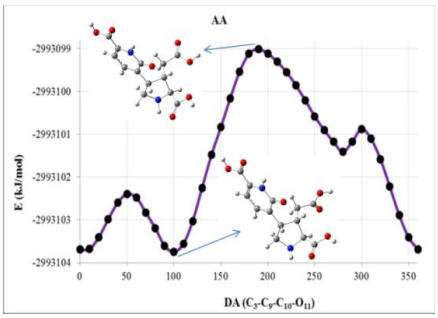

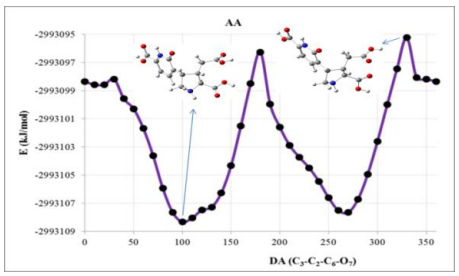

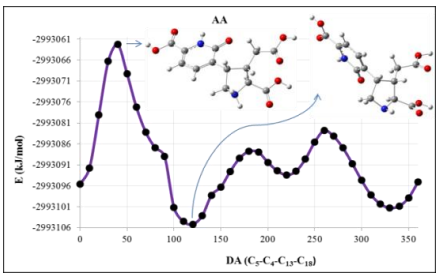

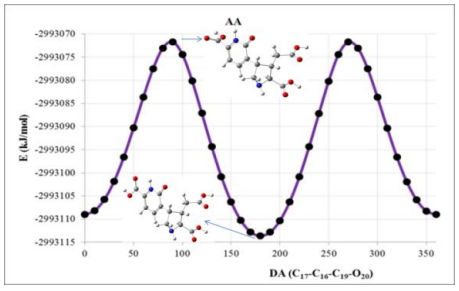

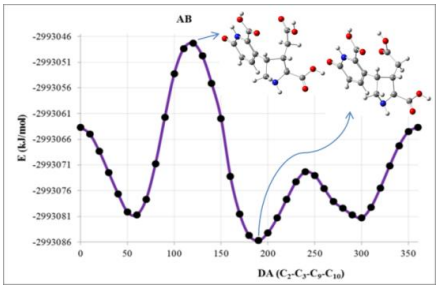

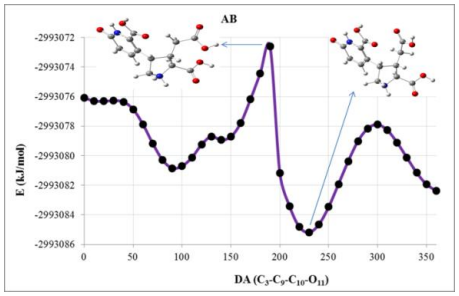

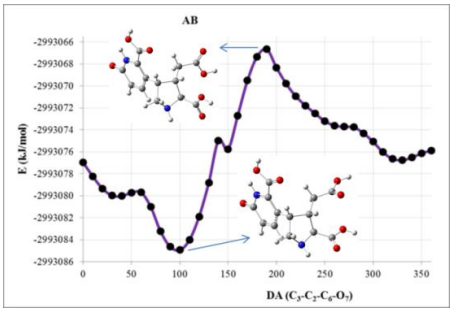

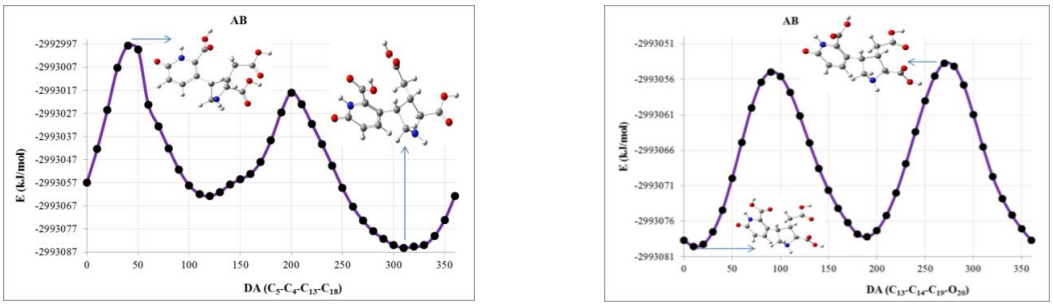

Figure 3: The PES scan of **AA** and **AB** as a function of selected dihedral angle and the structures corresponded to the maximum and minimum points.

Table **6** shows the characteristics (energies and dihedral angles) of the maximum and minimum points on the PES curves of **AA** and **AB**, and corresponding rotational barriers. According to the data presented in Table **6**, it is clear that by rotation of the heterocyclic ring located on C_4 around the C4–C13 bond (which corresponds to the φ dihedral angle), a significant increment in rotational energy is observed.

Table 6: The characteristics of maximum and minimum points of the PES curves, and rotational barrier for **AA** and **AB** obtained by B3LYP/6-31++G** method.[a]

Compound	Torsion angle and Energy	Maximum point	Minimum point	Rotational barrier
AA	α E	110 –2993077.1	190 –2993108.5	31.4
AA	β E	190 –2993098.7	100 –2993103.4	4.7
AA	γ E	330 –2993094.7	100 –2993107.8	13.1
AA	φ E	40 –2993061.8	120 –2993104.7	42.9
AA	θ E	90 (or 270) –2993071.7	180 –2993113.7	42.0
AB	α E	120 –2993046.8	190 –2993085.2	38.4
AB	β E	190 –2993072.6	230 –2993085.2	12.6
AB	γ E	190 –2993066.2	100 –2993084.4	18.2
AB	φ E	40 –2992997.7	310 –2993085.2	87.5
AB	θ E	270 (or 90) –2993053.8	10 –2993079.5	25.7

[a]All energies are in kJ/mol.

This trend can be attributed to the repulsive interactions between pyridone ring (along with corresponding functional groups) and adjacent atoms or groups. On the other hand by rotation of carboxyl group located on C_9 around the C_9–C_{10} bond (which corresponds to the β dihedral angle), we found the lowest amounts of rotational energy which may be justified in term of the absence of any significant repulsive interactions.

Conformational analysis concerning to the rotation around of C_{16}-C_{19} (for AA) and C_{14}-C_{19} (for AB) bonds, θ dihedral angle, shows a regular trend in the potential energy surface curves. Since at θ=90° and 270°, the C_{19}=O_{20} carbonyl group is completely perpendicular with respect to the pyridone ring, the resonance interactions are failed and the resulting conformers are energetically unstable whereas at θ=0° and 180°, due to the possibility of conjugation of C_{19}=O_{20} carbonyl group with adjacentπ system, reduction in potential energy surface is observed and corresponding conformers are energetically stable. A similar explanation can be provided for compound **AB** at φ=40° and 310° dihedral angles which coplanarity of C_{19}=O_{20} carbonyl group with pyridone ring is one of the important crucial factors.

The structures of lowest energy (**AA-l** and **AB-l**) and highest energy (**AA-h** and **AB-h**) conformers are presented in Figure **S3** of supporting information. In addition to the structures and thermodynamic parameters, the distance between interacting atoms and also the estimated hydrogen bond energy (E_{HB}, calculated by AIM calculations which demonstrated in Table **S5** of supplementary information) are also shown in Figure **S3**. Also their corresponding molecular graphs obtained by AIM calculations are illustrated in Figure **S4** of supplementary information.

The relevant structures and data calculated for compound **AA** and **AB** reported in Figure **S3** indicate that for most stable conformers, lower ΔH_f°, ΔG_f° and E_{tot} were obtained in comparison to unstable conformers. It is clear that intra-molecular hydrogen bond including N_1…H–C_{18} and O_{22}…H–C_9 for **AA** and N_1…H–C_{18}, O_{20}…H–C_4 and O_8…H–C_9 for **AB** are affected the stability of **AA-l** and **AB-l**, whereas steric or electronic repulsions (which are resulting from decrement of distance between interacting atoms to the less than the sum of van der Waals radii) such as C_5–H…H–C_{18}, O_8…C_{10} and O_{22}…C_9 interactions for **AA,** and C_5–H…H–C_{18} and O_8…C_{10}interactions for **AB** are responsible of the destabilization of **AA-h** and **AB-h** geometries.

Finally it may be stated that some determining factors such as intra-molecular hydrogen bond, steric or electronic repulsions and the possibility of resonance interaction between pyridone ring and carboxyl group attached to it, are affected the stability of **AA** and **AB** conformers.

Computational details:

All calculations were carried out using the Gaussian 09 program package [22]. B3LYP and M052X methods with 6-31++G** basis set have been used to carry out calculations of energies and geometry optimizations for the acromelic acid A and B. In order to verify the accuracy of calculations, the frequencies of the optimized geometries were calculated. For conformational analysis, Potential Energy Surfaces were calculated as a function of dihedral angles with B3LYP/6-31++G** method. Conductor-like Polarizable Continuum Model (CPCM) was applied for investigation of solvation effects on geometries. Charge density distributions have also been studied using natural bond orbital (NBO) analysis of Weinhold [23].

Conclusion

The B3LYP and M052X calculations in both gas phase and aqueous solution for Acromelic acid A and B indicated that structural, electronic and thermodynamic parameters are dependent on the pyridone ring located on the C_4 of pyrrolidine ring. AIM calculations indicated that due to the polar functional groups in **AA** and **AB**, intra-molecular hydrogen bond is one the most important determining factors of the geometry stability. The potential energies surfaces (PES) were calculated as function of different dihedral angles and most stable and unstable conformer were determined. The results obtained from PES and AIM calculations on most stable and unstable conformers were shown that some determining factors such as intra-molecular hydrogen bond, steric or electronic repulsions and the possibility of resonance interaction between pyridone ring and the carboxyl group attached to it, are affected the stability of conformers.

Acknowledgment

We are thankful to the Research Council and Office of Graduate Studies of the University of Ayatollah Alozma Borujerdi for their financial support.

References

[1] Konno, K.;Shirahama, H.; Matsumoto, T.*Tetrahedron Lett.***1983**, *24*, 939.

[2] Baldwin, J. E.; Fryer, A. M.; Spyvee, M. R.; Whitehead, R. C.; Wood, M. E. *Tetrahedron Lett.* **1996**, *37***,** 6923.

[3] Parsons, A.F.; *Tetrahedron***1996**, *52*, 4149.

[4] Konno, K.; Hashimoto, K.;Ohfune, Y.; Shirahama, H.; Matsumoto, T. *J. Am. Chem. Soc.***1988,** *110*, 4807.

[5] Higashi, T.; Isobe, Y.; Ouchi, H.; Suzuki, H.; Okazaki, Y.; Asakawa, T.; Furuta, T.; Wakimoto, T.; Kan, T. *Org. Lett.* **2011**, *13*, 1089.

[6] Ouchi, H.; Asahina, A.; Asakawa, T.; Inai, M.; Hamashima, Y.; Kan, T. *Org. Lett.***2014,** *16*, 1980.

[7] Taguchi, T.; Tomotoshi, K.; Mizumura, K. *Neuroscience Lett.***2009**, *456*, 69.

[8] Kanazawa, M.; Furuta, K.; Doi, H.; Mori, T.; Minami, T.; Ito, S.; Suzuki, M. *Bioorg. Med. Chem. Lett.* **2011**, *21*, 2017.

[9] Sun, P.; Wang, G. X.; Furuta, K.; Suzuki, M. *Bioorg. Med. Chem. Lett.* **2006**, *16*, 2433.

[10] Bunch, L.; Krogsgaard-Larsen, P. *Med. Res. Rev.* **2009,***29* , 3.

[11] Miyazaki, Sh.; Minami, T.; Mizuma, H.; Kanazawa, M.; Doi, H.; Matsumura, Sh.; Lu, J.; Onoe, H.; Furuta K.; Suzuki, M.; Ito, S. *Eur. J. Pharm.* **2013**, *710*, 120.

[12] Oe, K.; Ohfune, Y.; Shinada, T. *Org. Lett.* **2014**, *16*, 2550.

[13] Omoto, H.; Matsumura, Sh.; Kitano, M.; Miyazaki, Sh.; Minami, T.; Ito, S. *Eur. J. Pharm.* **2015**, *760*, 42.

[14] Memarian, H. R.; Soleymani, M.; Sabzyan, H.; Bagherzadeh, M.; Ahmadi, H. *J. Phys. Chem. A* **2011**,*115*, 8264.

[15] Soleymani, M. *Iran. J. Org. Chem.* **2016**, *8*, 1723, and references cited therein.

[16] Jönsson, P. G.; Kvick, A. *Acta Cryst.***1972**, *B28*, 1827.

[17] Price, W. D.; Jockusch, R. A.; Williams, E. R. *J. Am. Chem. Soc.***1997**, *119*, 11988.

[18] Espinosa, E.; Molins, E.; Lecomte, C. *Chem. Phys. Lett.* **1998**, *285*,170.

[19] Glendening, E. D.; Landis, C. R.; Weinhold, F. *Comput. Mol. Sci.***2012**, *2*, 1.

[20] Forlani, L.; Cristoni, G.; Boga, C.; Todesco, P. E.; Del Vecchio, E.; Selva, S.; Monari, M. *Arkivoc* **2002**, *XI*, 198.

[21] Schlegel, H. B.; Gund, P.; Fluder, E. M. *J. Am. Chem. Soc.***1982**, *104*, 5347.

[22] Frisch, M. J.; Trucks, G. W.; Schlegel, H. B.; Scuseria, G. E.; Robb, M. A.; Cheeseman, J. R.; Scalmani, G.; Barone, V.; Mennucci, B.; Petersson, G. A.; Nakatsuji, H.; Caricato, M.; Li, X.; Hratchian, H. P.; Izmaylov, A. F.; Bloino, J.; Zheng, G.; Sonnenberg, J. L.; Hada, M.; Ehara, M.; Toyota, K.; Fukuda, R.; Hasegawa, J.; Ishida, M.; Nakajima, T.; Honda, Y.; Kitao, O.; Nakai, H.; Vreven, T.; Montgomery, J. A.; Peralta, J. E.; Ogliaro, F.; Bearpark, M.; Heyd, J. J.; Brothers, E.; Kudin, K. N.; Staroverov, V. N.; Kobayashi, R.; Normand, J.; Raghavachari, K.; Rendell, A.; Burant, J. C.; Iyengar, S. S.; Tomasi, J.; Cossi, M.; Rega, N.; Millam, J. M.; Klene, M.; Knox, J. E.; Cross, J. B.; Bakken, V.; Adamo, C.; Jaramillo, J.; Gomperts, R.; Stratmann, R. E.; Yazyev, O.; Austin, A. J.; Cammi, R.; Pomelli, C.; Ochterski, J. W.; Martin, R. L.; Morokuma, K.; Zakrzewski, V. G.; Voth, G. A.; Salvador, P.; Dannenberg, J. J.; Dapprich, S.; Daniels, A. D.; Farkas, Ö.; Foresman, J. B.; Ortiz, J. V.; Cioslowski, J.; Fox, D. J. *Gaussian 09*, Gaussian, Inc.: Wallingford, CT, **2009**.

[23] Reed, A. E.; Curtiss, L. A.; Weinhold, F. *Chem. Rev.***1988**, *88*, 899.